

Multitask deep learning with spectral knowledge for hyperspectral image classification

Shengjie Liu, Qian Shi, and Zhixin Qi

Abstract—In this letter, we introduce multitask learning to hyperspectral image classification. Deep learning models have achieved promising results on hyperspectral image classification, but their performance highly rely on sufficient labeled samples, which are scarce on hyperspectral images. However, samples from multiple data sets might be sufficient to train one deep learning model, thereby improving its performance. To do so, spectral knowledge is introduced to ensure that the shared features are similar across domains. Four hyperspectral data sets were used in the experiments. We achieved better classification accuracies on three data sets (Pavia University, Indian Pines, and Pavia Center) originally with poor results or simple classification systems and competitive results on Salinas Valley data originally with a complex classification system. Spectral knowledge is useful to prevent the deep network from overfitting when the training samples were scarce. The proposed method successfully utilized samples from multiple data sets to increase its performance.

Index Terms—multitask learning, transfer learning, deep learning, convolutional neural network, hyperspectral image classification

I. INTRODUCTION

Remote sensing image classification, also known as semantic segmentation in computer vision, provides land use and land cover information that is essential for environment and urban management. Thus, many supervised algorithms have been proposed to accurately discriminate land cover classes in remote sensing images, including support vector machines, random forests, and neural networks [1]–[7]. Recently, deep learning, particularly deep convolutional neural networks (CNNs), has achieved considerable progress in remote sensing image classification, including hyperspectral image classification, and has achieved state-of-the-art results [8]–[14].

Hyperspectral data are rich in spectral information and thus have a high potential for land use and land cover mapping [2], [15]. For the semantic segmentation of hyperspectral images, a deep CNN will have more parameters if the input data have more spectral bands. For example, a deep contextual CNN for hyperspectral image classification was designed in [10]; the parameters varied from 613,000 (613K) for 103 bands to 1,876K for 224 bands. Although the performance of the deep CNN was promising, sufficient training samples

were needed to prevent the network with huge amounts of parameters from overfitting. However, collecting samples for hyperspectral data is time consuming and labor intensive, resulting limited labeled samples on hyperspectral images.

Several methods were proposed to tackle the dilemma between big networks and small samples. Some studies lightened the network by utilizing the 1×1 convolutional layers [16], [17]. [18] reduced the parameters by designing a simplified four layers network without hyperparameters, which applied an ensemble manner to utilize spatial-spectral information from hyperspectral data using 20 labeled samples per class. However, a deeper network with more parameters is expected to have a better performance. Thus, we should prevent overfitting as well as maintain the deepness and complexity of deep learning models by enlarging the training sample set.

One may consider transfer learning to leverage samples from external sources. For instance, [19] attempted to find new representations for each class from the source domain to the target domain by multiple linear transformations with low-rank reconstruction. [20] first trained a kernel machine with labeled data, which was then adapted to new data with manifold regularization. [21] proposed a kernel-based measure of data shift to select domain-invariant discriminant features for hyperspectral images. The aforementioned domain adaptation techniques successfully utilized samples from other source to increase models' generalization ability in the target domain. But they required the source and target data share an identical classification system, which limits the use of these methods. [22] applied the fine-tuning technique to extract spectral-spatial features from a CNN with two branches. In a fine-tuning fashion, they were able to use samples from data sets with diverse classification systems and from different sensors. In an unsupervised manner, [23] used self-taught learning on large amounts of unlabeled samples to learn CNN models (autoencoders) that were generalized enough to extract features for supervised classification with limited labeled samples. Although labeled samples are scarce on single hyperspectral image, a lot of hyperspectral data are available in the last two decades thanks to the development of hyperspectral imaging. Thus, if we can use labeled samples from multiple data sets in a supervised manner, we can solve the overfitting problem of deep CNN models.

In this letter, we propose a multitask deep learning method to leverage limited labeled samples from multiple data sets. Multitask learning is a type of transfer learning, but unlike fine tuning, multitask learning does not require the source data have a large quantity of training samples. Instead, we use samples from multiple data sets to cotrain one network,

Manuscript received XX XX, 2019; revised XX XX, 2019. This work was supported in part by FUNDING.

Shengjie Liu is with the Guangdong Provincial Key Laboratory of Urbanization and Geo-simulation, Sun Yat-sen University, Guangzhou 510275, China (e-mail: liushengjie0756@gmail.com).

Qian Shi and Zhixin Qi are with Guangdong Provincial Key Laboratory of Urbanization and Geo-simulation, School of Geography and Planning, Sun Yat-sen University, Guangzhou 510275, China (e-mail: shixi5@mail.sysu.edu.cn; qizhixin@mail.sysu.edu.cn).

thereby improving its generalization. The intuition of multitask learning is that two or multiple tasks share the similar features. For hyperspectral image classification, the spectral information has its physical meaning (radiance or reflectance) and is independent of the data set used. Therefore, utilizing samples among data sets with varying classification systems and even different sensors is possible.

The major contributions of this letter is summarized as follows.

- We propose a multitask deep learning model that can leverage limited samples from multiple data sets. Thus, the model has a better performance.
- Spectral knowledge is utilized in the network, providing a more robust multitask learning environment.

II. METHODOLOGY

A. Deep CNNs

Deep CNNs have achieved great success in hyperspectral image classification mainly because of two reasons. One is that it can generate spatial features from the input image by convolutional layers; the other is that the generated spatial features and the spectral features of the input image (the spatial-spectral features) are transformed nonlinearly into a high dimensional feature vector, from which the classifier can easily distinguish different classes. Therefore, the structure of a deep CNN can be seen as the combination of a feature extractor $\phi(\cdot)$ and a classifier $f(\cdot)$ (Fig. 1a). The shallow layers are treated as the feature extractor, while the last fully connected layer with the softmax function is treated as the classifier. For a input image sample x , a tensor with the shape of $H \times W \times C$ in our study (H, W , and C stand for height, width, and channels of the input image, respectively), the feature extractor $\phi(\cdot)$ extracts, fuses, and transforms the sample x to a feature vector x_ϕ that the classifier $f(\cdot)$ can better differentiate:

$$x_\phi = \phi(x). \quad (1)$$

The classifier $f(\cdot)$ takes the output vector x_ϕ from the feature extractor $\phi(\cdot)$ as its input. In a CNN, the fully connected layer with the softmax activation function serves as the classifier $f(\cdot)$ and gives the probability $P(y = j|x_\phi)$ of the j -th category:

$$P(y = j|x_\phi) = \frac{\exp(x_\phi^T w_j + b_j)}{\sum_{k=1}^K \exp(x_\phi^T w_k + b_k)}, \quad (2)$$

where w_j is the weight vector of the j -th neuron in the fully connected layer, b_j is a bias element corresponding to the j -th neural, and K is the number of category.

B. Multitask learning

Let X_t be the target instance space, where each instance $x_t \in X_t$ and t represents the target space. Given a labeled training data set with index i consisting of a few pairs (x_t^i, c_t^i) , where $x_t^i \in X_t$ and $c_t^i \in C_t = \{1, \dots, |c_t|\}$ is the class label of x_t^i . The classification task for the target data is to learn a deep CNN with a feature extractor $\phi_t(\cdot)$ and a predictive

function $f_t(\cdot)$ that can predict the corresponding label c_t of a new instance x_t . The classification task for the source data is the same – to learn a deep CNN with a feature extractor $\phi_s(\cdot)$ and a predictive function $f_s(\cdot)$.

When the training samples are limited in the target domain t , due to the large amount of parameters in the deep CNN $(\phi_t(\cdot), f_t(\cdot))$, especially in the feature extractor $\phi_t(\cdot)$, the model is easily over fitting, degrading its performance. To solve this problem, we can make use of samples from both the source domain and target domain to train a single deep CNN. This single deep CNN is referred to the multitask deep CNN. The basic theory behind multitask learning for hyperspectral image classification is that, samples from similar data sets should share some similar features (spatial or spectral) and thus can help the deep CNN to learn a more powerful feature extractor. In multitask deep CNN model, the feature extractor $\phi(\cdot)$ for both the source and target data is the same:

$$\phi(\cdot) = \phi_t(\cdot) = \phi_s(\cdot). \quad (3)$$

Thus, we can train a multitask deep CNN $(\phi(\cdot), f_s(\cdot), f_t(\cdot))$ for the source and target data. Now that the training samples are enlarged from different data sets, the performance of the model should be enhanced for both the data sets, especially the one with limited labeled samples.

For hyperspectral data, the spectral information has its physical meaning – representing the radiance or the reflectance of the ground target – and is independent of the data set used. Therefore, features from spectral information should be similar when two hyperspectral data sets have similar spectral range and bands. By using samples from multiple hyperspectral data sets, the deep learning model should improve its performance.

III. EXPERIMENTS

A. Hyperspectral Data Sets

Four hyperspectral data sets were used in the experiments. The first one is the Indian Pines (IN) data set with a size of $145 \times 145 \times 200$ captured by Airborne Visible/Infrared Imaging Spectrometer (AVIRIS) sensor over an agricultural area. There are 16 classes in this data. The second data set, Salinas Valley (SA), is also captured by AVIRIS sensor. It consists of a 512×217 agricultural area with 204 spectral bands and 16 classes. The third data set is the Pavia University (PU) data set with a size of $610 \times 340 \times 103$ and 9 classes. It was acquired by the Reflective Optics System Imaging Spectrometer (ROSIS) sensor over an urban area. The last one is the Pavia Center (PC) data set, captured by the ROSIS as well. It consists of 1096×715 pixels with 102 spectral bands and comprises 9 classes.

B. Experimental Setup

We implemented the multitask deep CNN using Keras with TensorFlow. The experiments were conducted on a machine equipped with a 3.0 GHz Intel Core i5-8500 CPU, 32G RAM, and an NVIDIA GeForce GTX1060 6G GPU. When training the multitask CNN, we used the AdaDelta optimizer with a batch size of 20. The learning rate was set as 1.0 for multitask learning in the first 100 epochs. Then, the learning rate was

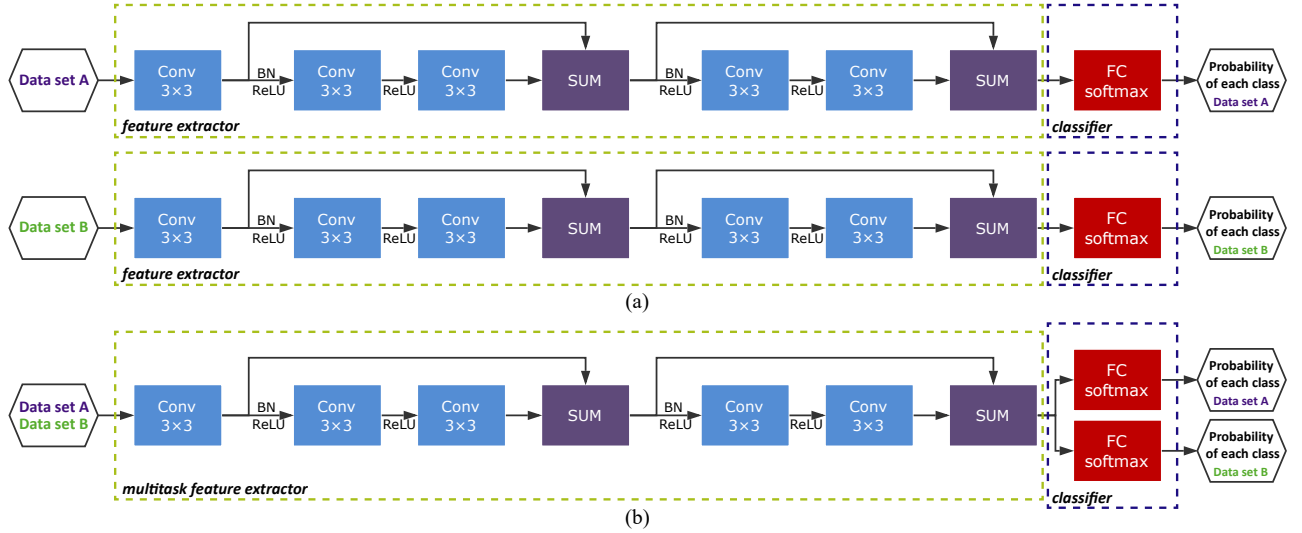


Fig. 1. The architecture of the (multitask) deep CNN used in this study. (1) Deep CNN for single data set. (2) Multitask deep CNN for multiple data sets.

set as 0.1 to adjust to each task for 30 epochs. The final classification was voted from five predictions, which were obtained from the end of training in a step of two epochs. With the spectral knowledge, the first convolutional layer is weight sharing; without the spectral knowledge, each data set has its own weights of the first convolutional layer. All the data were augmented 4 times by mirroring each sample horizontally, vertically, and diagonally.

C. Experiments on the ROSIS data sets

In the first group of experiments, we conducted multitask learning on the ROSIS data sets. Although the ROSIS data sets are from the same sensor, they were preprocessed individually, resulting a scene (Pavia Center) with 102 bands and the other (Pavia University) with 103 bands. To align the spectral bands, the last band of Pavia Center was repeated, so the input channels is 103. We used bands from 11 to 113 from the AVIRIS data sets when they were involved to train the ROSIS data sets. The classification results of Pavia University are presented in Table I. Compared with the baseline, multitask learning generated results with higher overall accuracies in all cases. Multitask learning with Pavia Center and multitask learning with another data set with a different sensor did not significantly affect its performance, indicating the robustness of multitask learning. When spectral knowledge was involved, the multitask model generalized better with fewer training samples. The results of Pavia Center are presented in Table II. This data set is easily to classify, achieving over 95% overall accuracy with only 5 samples per class. Nevertheless, it achieved better classification results using multitask learning with the Salinas Valley data set. Its performance was inline with or was slightly degraded when it was cotrained with other data.

For illustrate purposes, we show the classification maps with different methods in Fig. 2 using 10 labeled samples per class. Compared with the baseline, classification maps generated by multitask learning are more smooth, especially the one

cotrained with Salinas Valleys. Nevertheless, the classification maps need improvement as they are too fragmented.

D. Experiments on the AVIRIS data sets

In the second group of experiments, we conducted multitask learning on the AVIRIS data sets. For the Salinas Valley data set, only the last 160 spectral were applied in the experiments to reduce the atmospheric effects. For the Indian Pines data set, only the last 160 spectral bands were used in the experiments as well. When the ROSIS data sets were involved, we repeated the last 57 spectral bands for Pavia University and the last 58 spectral bands for Pavia Center, respectively. In this case, the spectral information is mismatched among data sets. The classification results of Indian Pines are represented in Table III. The overall accuracy was slightly improved, from 39.17% to 42.44% with 5 samples per class to 70.76% to 73.66% with 30 samples per class. In this task, results cotrained with Salinas Valley were the best among all the methods, mainly because they came from the same sensor. Finally, the classification results of Salinas Valley were represented in Table IV. Only on this data set that we observe a dramatic decrease in overall accuracy with multitask learning. It might be that this data set has the most complex classification system with 16 classes and a relatively high classification performance. The spectral knowledge from other data sets is hard to help such a classification task.

IV. CONCLUSION

This letter investigates multitask deep learning for hyper-spectral image classification. By cotraining a deep network from multiple data sets, the overfitting problems in deep learning models can be reduced. The experimental results demonstrate that, multitask learning is particularly useful in data sets with poor accuracies and simple classification systems. Future studies should work on how to maintain the performance on data sets with relatively high classification performance when using multitask learning.

TABLE I
OVERALL ACCURACY OF PAVIA UNIVERSITY.

NoS/class	Baseline	MTL w/ spectral knowledge				MTL w/o spectral knowledge		
each domain	-	PC	SA	IN	ALL	PC	SA	IN
5	62.80±7.03	66.11±6.30	64.78±3.00	64.84±7.04	65.66±6.85	64.25±5.31	64.54±5.80	64.45±7.18
10	72.46±4.07	75.11±3.22	75.07±4.37	74.78±5.49	75.88±4.76	74.83±4.56	74.39±3.87	74.58±3.57
15	80.75±2.72	82.71±3.42	83.92±2.43	82.48±3.30	83.09±2.71	83.55±2.92	83.53±3.56	82.08±3.61
20	84.67±1.87	86.72±1.99	86.93±1.44	86.18±1.62	85.71±1.38	86.07±2.01	87.15±1.65	86.42±1.41
25	87.39±1.51	88.88±1.43	89.53±1.16	89.09±1.82	88.21±0.93	89.20±1.07	89.30±1.46	88.61±1.09
30	87.49±1.31	89.82±1.41	90.44±1.41	90.68±1.16	88.59±1.21	90.28±1.27	90.23±1.62	90.21±1.20

TABLE II
OVERALL ACCURACY OF PAVIA CENTER.

NoS/class	Baseline	MTL w/ spectral knowledge				MTL w/o spectral knowledge		
each domain	-	PU	SA	IN	ALL	PU	SA	IN
5	95.20±1.66	94.39±1.86	96.30±1.79	95.59±0.91	93.01±2.73	95.52±1.70	96.01±1.98	95.05±2.13
10	96.59±1.01	95.95±1.40	97.26±0.61	96.83±0.50	95.92±0.75	96.73±0.79	97.02±0.77	96.56±1.11
15	97.46±0.23	97.26±0.29	97.64±0.23	97.40±0.22	96.95±0.46	97.45±0.39	97.54±0.32	97.39±0.23
20	97.65±0.37	97.50±0.344	97.73±0.26	97.66±0.23	97.17±0.32	97.70±0.35	97.75±0.27	97.70±0.24
25	97.82±0.31	97.72±0.29	97.90±0.23	97.81±0.22	97.53±0.21	97.91±3.55	97.88±0.29	97.88±0.24
30	98.02±0.20	97.92±0.23	98.18±0.22	97.95±0.20	97.71±0.28	98.14±0.22	98.20±0.25	97.97±0.23

TABLE III
OVERALL ACCURACY OF INDIAN PINES.

NoS/class	Baseline	MTL w/ spectral knowledge				MTL w/o spectral knowledge		
each domain	-	SA	PC	PU	ALL	SA	PC	PU
5	39.17±3.06	42.44±3.24	41.09±3.77	40.26±2.95	41.54±3.20	36.17±5.08	40.31±3.49	39.59±3.10
10	48.09±3.32	53.61±3.97	53.73±3.23	52.28±3.46	53.27±3.31	54.62±3.25	52.61±4.88	49.21±4.56
15	56.95±3.42	61.41±3.42	60.99±2.67	59.67±2.83	59.62±1.28	62.18±1.29	60.22±3.66	59.75±2.95
20	64.54±1.98	67.73±1.86	66.25±2.20	64.46±1.99	66.11±2.11	66.53±1.69	60.29±3.47	66.13±2.14
25	68.17±1.32	70.83±1.93	69.97±2.10	68.04±1.62	70.57±2.02	71.33±2.72	69.76±2.06	69.50±1.70
30	70.76±2.07	73.66±1.11	72.50±0.86	71.35±1.26	72.66±1.42	72.69±1.75	71.80±1.59	72.60±1.17

TABLE IV
OVERALL ACCURACY OF SALINAS VALLEY.

NoS/class	Baseline	MTL w/ spectral knowledge				MTL w/o spectral knowledge		
each domain	-	IN	PC	PU	ALL	IN	PC	PU
5	80.29±2.76	71.15±2.75	76.75±2.66	72.30±4.02	70.86±2.78	77.63±3.66	79.60±2.04	77.57±3.87
10	81.29±1.98	77.78±1.55	79.58±1.71	76.60±2.32	76.33±1.09	80.03±1.95	80.57±1.25	79.72±1.37
15	82.84±2.38	80.77±1.22	82.24±1.86	80.15±2.07	79.96±1.11	81.54±2.81	82.34±2.37	81.82±2.05
20	83.78±1.90	82.27±0.93	82.95±1.41	82.29±1.57	82.29±1.34	84.16±2.14	84.09±1.48	83.32±1.41
25	85.11±2.03	83.27±1.39	84.23±1.65	83.27±1.69	83.74±1.25	84.29±1.61	84.37±1.59	83.91±1.56
30	85.63±1.80	84.70±1.43	85.29±1.18	84.02±1.15	84.27±1.34	85.21±1.46	85.96±1.97	84.86±1.80

ACKNOWLEDGMENT

The authors would like to thank Prof. D. Landgrebe for making the AVIRIS Indian Pines hyperspectral data set available to the community and Prof. P. Gamba for providing the ROSIS data over Pavia, Italy, along with the training and test set.

REFERENCES

- [1] T. Yoshida and S. Omatu, "Neural network approach to land cover mapping," *IEEE Transactions on Geoscience and Remote Sensing*, vol. 32, no. 5, pp. 1103–1109, 1994.
- [2] F. Melgani and L. Bruzzone, "Classification of hyperspectral remote sensing images with support vector machines," *IEEE Transactions on geoscience and remote sensing*, vol. 42, no. 8, pp. 1778–1790, 2004.
- [3] J. Ham, Y. Chen, M. M. Crawford, and J. Ghosh, "Investigation of the random forest framework for classification of hyperspectral data," *IEEE Transactions on Geoscience and Remote Sensing*, vol. 43, no. 3, pp. 492–501, 2005.
- [4] G. Mountrakis, J. Im, and C. Ogole, "Support vector machines in remote sensing: A review," *ISPRS Journal of Photogrammetry and Remote Sensing*, vol. 66, no. 3, pp. 247–259, 2011.
- [5] Z. Qi, A. G. O. Yeh, X. Li, and Z. Lin, "A novel algorithm for land use and land cover classification using RADARSAT-2 polarimetric SAR data," *Remote Sensing of Environment*, vol. 118, pp. 21–39, 2012. [Online]. Available: <http://dx.doi.org/10.1016/j.rse.2011.11.001>
- [6] S. Moustakidis, G. Mallinis, N. Koutsias, J. B. Theocharis, and V. Petridis, "Svm-based fuzzy decision trees for classification of high spatial resolution remote sensing images," *IEEE Transactions on Geoscience and Remote Sensing*, vol. 50, no. 1, pp. 149–169, 2012.
- [7] Y. Chen, Z. Lin, X. Zhao, G. Wang, and Y. Gu, "Deep learning-based classification of hyperspectral data," *IEEE Journal of Selected Topics in Applied Earth Observations and Remote Sensing*, vol. 7, no. 6, pp.

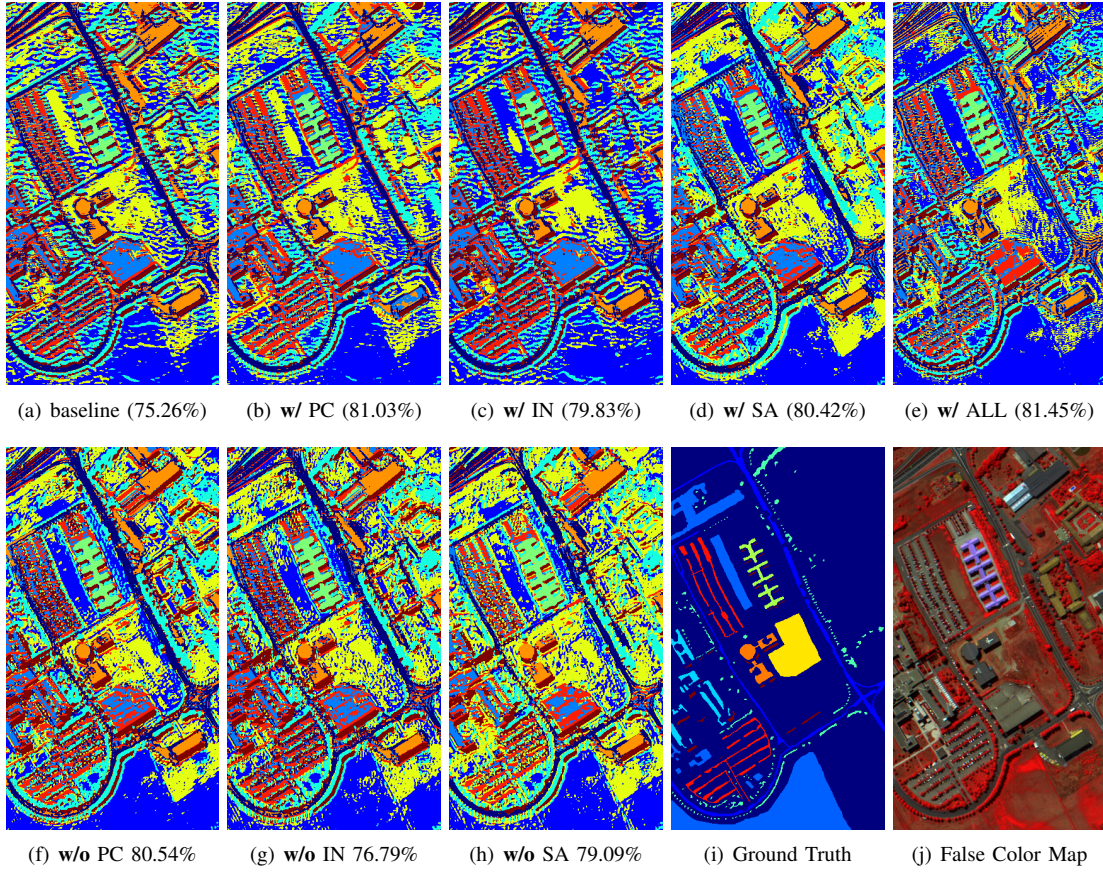


Fig. 2. Classification maps of Pavia University. **w/** represents with multitask learning with spectral knowledge, whereas **w/o** represents multitask learning without spectral knowledge. PC, IN, and SA indicate Pavia Center, Indian Pines, and Salinas Valley, respectively. ALL indicates multitask learning with all the available data sets.

- 2094–2107, 2014.
- [8] T.-H. Chan, K. Jia, S. Gao, J. Lu, Z. Zeng, and Y. Ma, “Pcanet: A simple deep learning baseline for image classification?” *IEEE Transactions on Image Processing*, vol. 24, no. 12, pp. 5017–5032, 2015.
 - [9] W. Zhao and S. Du, “Spectral–spatial feature extraction for hyperspectral image classification: A dimension reduction and deep learning approach,” *IEEE Transactions on Geoscience and Remote Sensing*, vol. 54, no. 8, pp. 4544–4554, 2016.
 - [10] H. Lee and H. Kwon, “Going Deeper with Contextual CNN for Hyperspectral Image Classification,” *IEEE Transactions on Image Processing*, vol. 26, no. 10, pp. 4843–4855, 2017.
 - [11] Z. Zhong, J. Li, Z. Luo, and M. Chapman, “Spectral–spatial residual network for hyperspectral image classification: A 3-d deep learning framework,” *IEEE Transactions on Geoscience and Remote Sensing*, vol. 56, no. 2, pp. 847–858, 2018.
 - [12] J. M. Haut, M. E. Paoletti, J. Plaza, J. Li, and A. Plaza, “Active learning with convolutional neural networks for hyperspectral image classification using a new bayesian approach,” *IEEE Transactions on Geoscience and Remote Sensing*, no. 99, pp. 1–22, 2018.
 - [13] B. Huang, B. Zhao, and Y. Song, “Urban land-use mapping using a deep convolutional neural network with high spatial resolution multispectral remote sensing imagery,” *Remote Sensing of Environment*, vol. 214, pp. 73–86, 2018.
 - [14] C. Zhang, I. Sargent, X. Pan, H. Li, A. Gardiner, J. Hare, and P. M. Atkinson, “An object-based convolutional neural network (ocnn) for urban land use classification,” *Remote sensing of environment*, vol. 216, pp. 57–70, 2018.
 - [15] G. Camps-Valls, D. Tuia, L. Bruzzone, and J. A. Benediktsson, “Advances in hyperspectral image classification: Earth monitoring with statistical learning methods,” *IEEE Signal Processing Magazine*, vol. 31, no. 1, pp. 45–54, 2014.
 - [16] M. Paoletti, J. Haut, J. Plaza, and A. Plaza, “A new deep convolutional neural network for fast hyperspectral image classification,” *ISPRS Journal of Photogrammetry and Remote Sensing*, vol. 145, pp. 120–147, 2018.
 - [17] S. Liu, H. Luo, Y. Tu, Z. He, and J. Li, “Wide contextual residual network with active learning for remote sensing image classification,” in *IGARSS 2018 - 2018 IEEE International Geoscience and Remote Sensing Symposium*, July 2018, pp. 7145–7148.
 - [18] B. Pan, Z. Shi, and X. Xu, “Mugnet: deep learning for hyperspectral image classification using limited samples,” *ISPRS Journal of Photogrammetry and Remote Sensing*, vol. 145, pp. 108–119, 2018.
 - [19] Q. Shi, B. Du, and L. Zhang, “Domain adaptation for remote sensing image classification: A low-rank reconstruction and instance weighting label propagation inspired algorithm,” *IEEE Transactions on Geoscience and Remote Sensing*, vol. 53, no. 10, pp. 5677–5689, 2015.
 - [20] W. Kim and M. M. Crawford, “Adaptive classification for hyperspectral image data using manifold regularization kernel machines,” *IEEE Transactions on Geoscience and Remote Sensing*, vol. 48, no. 11, pp. 4110–4121, 2010.
 - [21] C. Persello and L. Bruzzone, “Kernel-Based Domain-Invariant Feature Selection in Hyperspectral Images for Transfer Learning,” vol. 54, no. 5, pp. 2615–2626, 2016.
 - [22] J. Yang, Y.-Q. Zhao, and J. C.-W. Chan, “Learning and transferring deep joint spectral–spatial features for hyperspectral classification,” *IEEE Transactions on Geoscience and Remote Sensing*, vol. 55, no. 8, pp. 4729–4742, 2017.
 - [23] R. Kemker and C. Kanan, “Self-Taught Feature Learning for Hyperspectral Image Classification,” *IEEE Transactions on Geoscience and Remote Sensing*, vol. 55, no. 5, pp. 2693–2705, 2017.